VNU Journal of Science: Mathematics – Physics, Vol. xx, No. x (20xx) xx-xx

VNU Journal of Science: Mathematics - Physics

Journal homepage: https://js.vnu.edu.vn/MaP

Original Article

Analysis of the Structure and Luminescence Properties of $Sr_3Y_2Ge_3O_{12}$:0.05Eu^{3+} (SYGO:Eu^{3+}) According to Judd–ofelt Theory

Nguyen Mai Cao Hoang Phuong Lan[1], Nguyen Duc Trung Kien[1],
Cao Xuan Thang[1,*], Nguyen Viet Tung[1,2]

[1]International Training Institute for Materials Science (ITIMS),
Hanoi University of Science and Technology (HUST), 1, Dai Co Viet, Hanoi, Vietnam
[2]Institute of Science and Technology, Ministry of Public Security,
100 Chien Thang, Hanoi, Vietnam

Received 03 January 2023
Revised 11 March 2023; Accepted 13 March 2023

Abstract: In this report, SYGO:Eu^{3+} red phosphor have been successfully synthesized by sol-gel method. The X-ray diffraction results show that the sample has a cubic crystal structure, belonging to the space group Ia3d (230) without any doping. Scanning electron microscopy (FE-SEM) combined with EDS was performed to determine the microstructure and elemental composition of the fabricated phosphor. The particles are significantly agglomerated and are about ~200 nm in size. The results of fluorescence property investigation (PLE-PL) show that, the maximum emission spectrum at 612 nm under ultraviolet light close to 395 nm for excitation. Calculating the J-O intensity parameters, the result is that Ω_2 is larger than Ω_4 which proves that the surrounding local structure of the doped ion is asymmetric. In addition, the luminescence efficiency approximately calculation is 70%. Phosphor SYGO:Eu^{3+} has been fabricated which can be used as a solid lighting material for WLED.

Keywords: $Sr_3Y_2Ge_3O_{12}$:Eu^{3+}, Hydrothermal method, J-O theory, phosphors.

---

[*] Corresponding author.
E-mail address: thang.caoxuan@itims.edu.vn

https//doi.org/10.25073/2588-1124/vnumap.4800

1. Introduction

Over the years, in order to improve light efficiency, there were many of the research and development of white light-emitting diodes (WLEDs) which has attracted considerable attention. This is due to the relatively high luminous efficiency, low power consumption and reliability of WLED [1-3]. As is known, WLED is produced using a near-ultraviolet (NUV) or blue light-converting phosphor [4]. In particular, WLED widely used today is a combination of blue light-emitting GaN chip (450 nm) and a mixture of yellow phosphorus (555 nm), $Y_3Al_5O_{12}$:Ce^{3+} (YAG). The combination of these two phosphors results in a high color temperature (CCT > 6000 K) and a low color rendering index (CRI < 80) which is due to a lack of red and blue emitters. Therefore, research efforts are still needed to create WLED-applicable phosphors that meet the requirements of low correlated color temperature CCT and high color rendering index (CRI).

Another ways to get white LEDs shows high CRI which it was injected the red, green, and blue tricolor phosphor with the NUV chip (360-410 nm). The three-color phosphor used in this study is Y_2O_2S: Eu^{3+} for red, ZnS (Cu^{2+}, Al^{3+}) for green, and $BaMgAl_{10}O_{17}$: Eu^{2+} for blue [5]. Y_2O_2S: Eu^{3+} illustrates the information about the unstable chemical due to the release of sulfide gas is also dangerous to humans [6, 7]. The SYGO crystal structure belonging to the garnet form is known as a material with advanced properties such as structural, physical, chemical, and thermal properties [8-10].

Currently, there have been significant studies on the luminescence properties of phosphor SYGO:Eu^{3+} which gives red emission [11-13]. However, to the best of our knowledge, the optical properties of SYGO:Eu^{3+} as explained by J–O theory has not been evaluated yet.

By J-O theory, it is possible to clearly explain the behavior of rare earth ions when doped into the host lattice [14, 15]. It is a advanced analyzing the f-f absorption spectrum of Lanthan group elements. This quantum theory allows the determination of the intensity parameters Ω_λ ($\lambda = 2, 4, 6$) of rare-earth ions in crystal and many other physical quantities related to electronic displacement. The J-O intensity parameters of Eu^{3+} ions in the SYGO background matrix, and the binding-related changes were also elucidated. Besides studying the optical properties of SYGO: Eu^{3+} phosphor, we also investigated the structure through relevant measurements such as XRD, FE-SEM, EDS and decay time spectra.

2. Experimental

2.1. Materials

SYGO and SYGO:0.05 Eu^{3+} phosphor was synthesized by the sol-gel method. High purity input chemicals (Sigma-Aldrich Co.) such as strontium nitrate ($Sr(NO_3)_2$), yttrium nitrate hexahydrate ($Y(NO_3)_3$. $6H_2O$), germanium oxide (GeO_2), europium oxide (Eu_2O_3), citric acid ($C_6H_8O_7$), and polyethylene glycol (PEG) ($(C_2H_4O)_n$. H_2O) were weighed according to the ratio of the general formula $Sr_3Y_2Ge_3O_{12}$.

2.2. Synthesis

Firstly, GeO_2 was dissolved in nitric acid solution until a homogeneous solution was obtained. Then, de-ionized (DI) water was poured into the obtained solution to get germanium nitrate solution (solution I). Yttrium nitrate, strontium nitrate, and europium oxide are dissolved in DI water in solution II. To completely dissolve the two initial solutions, stir them for several times. After the chemical has completely disolved, the solution I was added slowly to the solution II. Then, a 16 mol of citric acid was added to the above solution mixture (the molar ratio of citric acid to the total number of metal ions in the matrix is 16:1). At last, a cross-linking agent (PEG) was added, and the mixture was agitated for 1 h to achieve a totally homogeneous solution. Furthermore, the stable metal complex mixture solution was heat with magnetic the stirrer for about 2 h at 85 °C. The solution combination and leave it at the same temperature for another 8 h. The solution slowly evaporates, leaving a brown wet gel. The wet gel was initially dried at 120 °C for 24 h in ambient atmosphere then annealed at 1200 °C for 8 h to get the phosphor samples which can be used for further analysis.

2.3. Characterizations

The crystalline phase structure of the sample was characterized by X-ray diffraction (XRD, D8 Advance, Bruker, Germany) with Cu-Ka radiation (λ =1.5418 Å) and (2θ=10–70°). The morphologies of samples were illustrated by field emission scanning electron microscopy (JEOL, JSM-6700 F, JEOL Techniques, Tokyo, Japan) accompanied with an energy dispersive spectroscopy (EDS) to examine the chemical composition. The optical properties of the Eu^{3+} doped SYGO were tested by NANO LOG spectrofluorometer (Horiba, USA) equipped with 450W Xe arc lamp and double excitation monochromators were used.

3. Results and Discussion

3.1. Crystal Structure

The result of Rietveld refinement of the SYGO host lattice and SYGO: $0.05Eu^{3+}$ phosphor is shown in Fig. 1. The refinement results demonstrate that the experimentally measured diffraction intensity agrees well with the theory, and there is no significant difference between the two lines. It is clearly that all the diffraction peaks give the detail pure cubic crystal phase of the structure's garnet with a space group of Ia3d (230) and match well with JCPDS # 85-2410 card. The cell parameters a = b = c = 13.20, $\alpha = \beta = \gamma = 90°$, and V = 2298.28 Å^3. The lattice constant a value of the SYGO host lattice (a = 13.06) and SYGO: $0.05Eu^{3+}$ phosphor (a = 13.22) was calculated based on the formula $1/d^2 = (h^2 + k^2 + l^2) / a^2$ for cubic structures. The lattice constant obtained approximate values from those reported in the standard card JCPDS # 85-2410 (a = 13.08) [12].

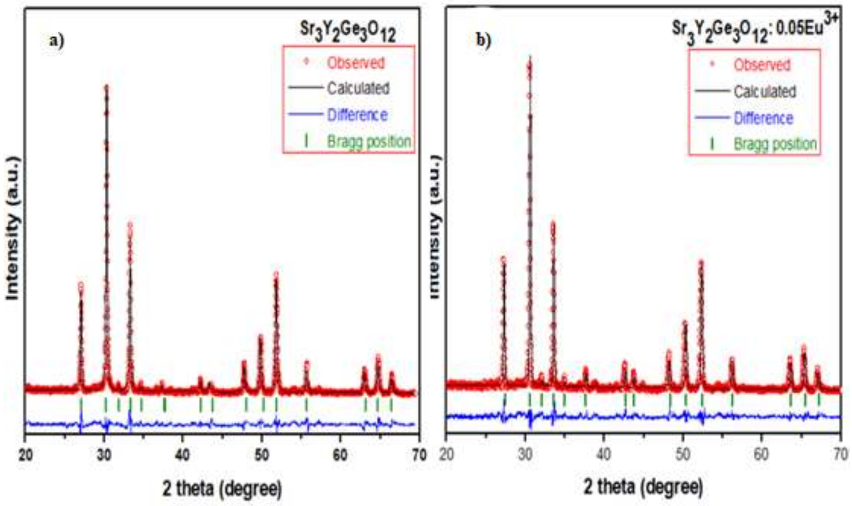

Figure 1. XRD Rietveld refinement of a) SYGO and b) SYGO:$0.05Eu^{3+}$.

3.2. Morphological Structure and Elemental Composition

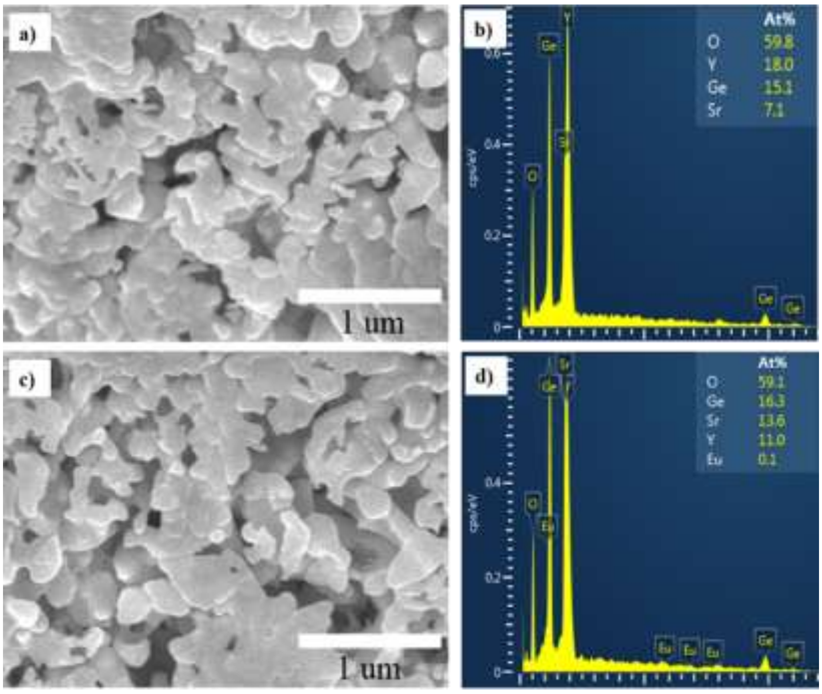

Figure 2. (a, c) FE-SEM image and (b, d) EDX spectrum of samples SYGO and SYGO:0.05Eu^{3++}.

FE-SEM images are used to characterize the micro-morphologies of the SYGO host lattice and SYGO: 0.05 Eu^{3+} (Fig. 2a, c). The samples were all granular, uneven, and a few micrometers in size, and the addition of Eu^{3+} had no effect on their morphology. Elemental mapping samples revealed no contaminant ions in the manufactured samples, indicating that phosphorus samples have been synthesized with high purity (Fig. 2b,d), respectively.

3.3. Photoluminescence Properties

Fig. 3a shows the PL excitation (PLE) spectra of the SYGO host lattice synthesized by the sol-gel method. The host lattice has the maximum absorption intensity at 270 nm. This region corresponds to the bound electron transfer absorption (CTB) in the SYGO host lattice.

Fig. 3b is the PL emission spectra of the SYGO host lattice synthesized by the sol-gel heating method at 1200 ^{o}C for 8 h. The emission at 720 nm observed in this method can be explained by the recombination of electron-hole pairs related to internal defects, defects of the SYGO host lattice (intrinsic defects) or errors surface damage inherent to very high densities of nanocrystals. The origin of this emission is thought to be due to the energy transfer from the non-agglutinating oxygen centers (NBOHs) to the oxygen vacancy (V_O) sites in the SYGO host lattice [16].

Fig.3c shows excitation and emission spectrum of SYGO:Eu^{3+}. It is clearly seen that the excitation spectrum includes peaks in the 260–500 nm range, which is attributed to the transition within the configuration (f – f) of Eu^{3+}. Peaks in the 250–350 nm range are attributed to the charge transfer band (CTB) [17], a series of excitation peaks at 377, 395, 414 and 466 nm mainly due to characteristic absorption transitions of the ground state $^7F_0$ of Eu^{3+} ions are $^7F_0 \rightarrow {}^5G_4$, $^7F_0 \rightarrow {}^5L_6$ and $^7F_0 \rightarrow {}^5D_3$ and $^7F_0 \rightarrow {}^5D_2$ [18]. The Fig.3d illustrated emission spectra of the SYGO:Eu^{3+} phosphors excited at 395 nm.

The spectrum includes emission peaks around 591, 612, 646 and 696 nm due to the $^5D_0 \rightarrow {}^7F_1$, $^5D_0 \rightarrow {}^7F_2$, $^5D_0 \rightarrow {}^7F_3$ and $^5D_0 \rightarrow {}^7F_4$ transitions of Eu^{3+} ions, respectively [19]. In which, the emission peak at 591 nm ($^5D_0 \rightarrow {}^7F_1$) is the magnetic dipole transition and the peak at 612 nm ($^5D_0 \rightarrow {}^7F_2$) is the forced electric dipole transition. The decay times of the samples were monitored at 612 nm emission and the excitation at 395 nm was measured.

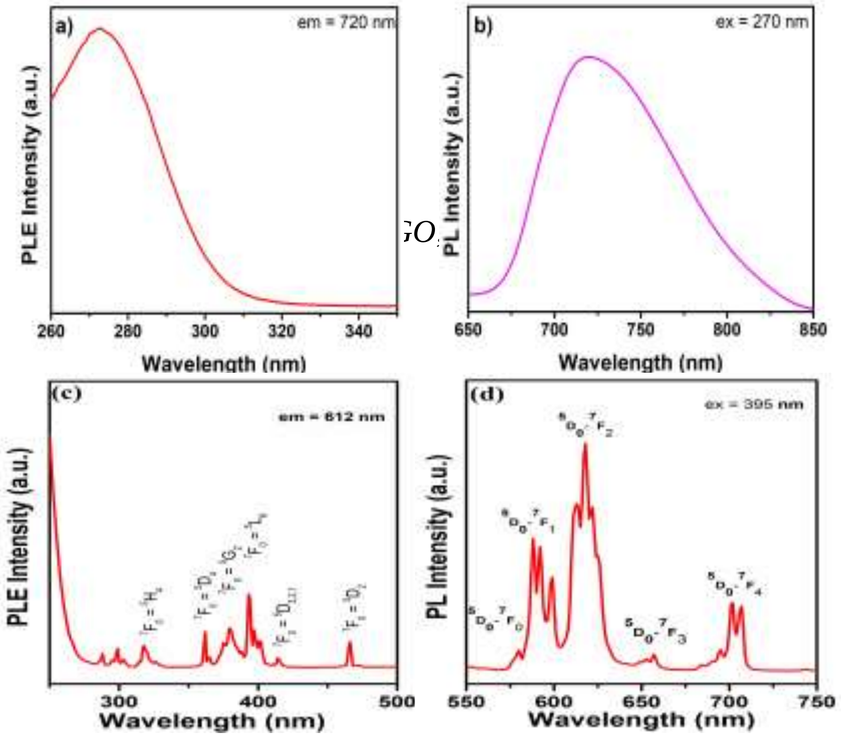

Figure 3. PLE-PL of (a,b)SYGO; (c,d) SYGO:Eu^{3+} host lattice.

Fig. 4 shows the decay curves of phosphor SYGO: $0.05Eu^{3+}$, the decay time (τ) can be calculated by the following formula [20]: $y(x) = A\exp(-x/\tau)$

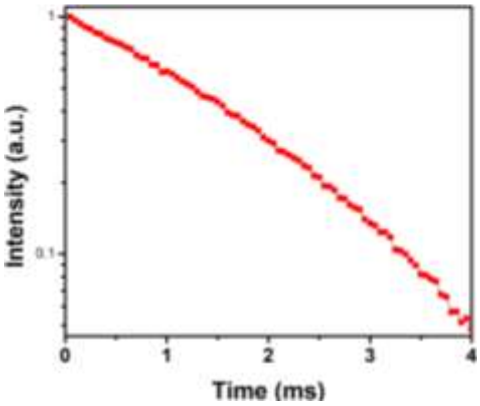

Figure 4. Decay time of SYGO:$0.05Eu^{3+}$.

where y(x) is the PL intensity at time x after the excitation light is turned off, A are the parameters representing fractions of the normalized PL intensity, and τ is the decay time. The calculation shows that the decay time is $\tau = 1.93$ ms.

Schematic representation of photophysical processes in Eu^{3+}-doped SYGO phosphor: The energy level mechanism for the luminescence participation process of Eu^{3+} ions are shown in Fig.5. With an excitation of 3950 nm, the electrons of the Eu^{3+} ion go from the CTB state and then decay to the ^5D_n level (n=0, 1, 2...) of the Eu^{3+} ion. Then, the electrons of the Eu^{3+} ion recombine with the hole at energies lower than ^5F_n (n=1-6), resulting in light.

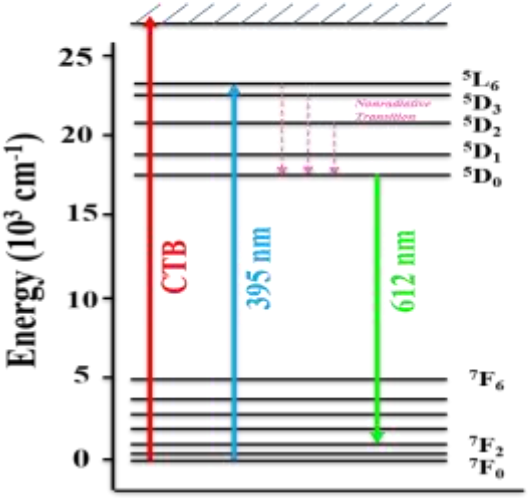

Figure 5. Energy level diagram of the Eu^{3+} ion in the SYGO host lattice.

3.4. Judd–Ofelt Calculations

The emission spectra consisted of typical emission bands of Eu^{3+} ions at 590, 612, and 699 nm corresponding to the transition from $^5D_0$ to ^7F_J, namely, $^5D_0 \rightarrow {}^7F_1$, $^5D_0 \rightarrow {}^7F_2$, and $^5D_0 \rightarrow {}^7F_4$ (Fig 3d). The $^5D_0 \rightarrow {}^7F_1$ displacement with the magnetic dipole (the vibration force of magnetic dipole motion is independent of the surrounding environment of the doped ion) and three $^5D_0 \rightarrow {}^7F_{2,4,6}$ displacements for electric dipoles (these electric dipoles are prohibited according to Laporte selection rule). According to JO theory, the calculated oscillator strength for an induced electric dipole transition from the ground state to an excited state.

$$f = \frac{8\pi^2 mc\nu}{h(2J+1)} \times \frac{(n^2+2)^2}{9n} \sum_{\lambda=2,4,6} \Omega_\lambda | < \Psi J ||U^\lambda|| \Psi' J' > |^2 \quad (1)$$

$$\frac{A_R(^5D_0 \rightarrow {}^7F_{2,4,6})}{A_R(^5D_0 \rightarrow {}^7F_1)} = \frac{S(^5D_0 \rightarrow {}^7F_{2,4,6})}{S(^5D_0 \rightarrow {}^7F_1)} = \frac{64\pi^4 e^2 v^3}{3h(2J+1)} \left(\frac{n(n^2+2)^2}{9} \right) \Omega_J (||U^J||)^2 \quad (2)$$

where *m* is the mass of the electron, v (cm^{-1}) is the wave number of the transition, *h* is Planck's constant, *e* is the charge of the electron and *n* is the refractive index of the material ($n_{SYGO} = 1$), J is the total angular momentum of the ground state, Ω_λ is the J-O intensity parameters, $||U^\lambda||^2$ are the doubly reduced matrix elements evaluated in the term unit tensor operator λ (λ = 2, 4, 6). The reduced matrix elements of Eu^{3+} ions are shown in Table 1 [21] were applied, and $J = 0$ for $^5D_0$ state emission. The parameters Ω_2 and Ω_4 can be easily estimated Eq. (1) and show in Table 2. Ω_2 depends on the relocation of $^5D_0 \rightarrow {}^7F_2$.

$\Omega_{4,\,6}$ depends on $^5D_0 \rightarrow {}^7F_{4,\,6}$ shifts. However, because $^5D_0 \rightarrow {}^7F_6$ was very weak, it was not observed during the experiments. Hence, Ω_6 was ignored.

Table 1. Squared reduced matrix elements

Transition form	$\|\|U^2\|\|^2$	$\|\|U^4\|\|^2$	$\|\|U^6\|\|^2$
$^5D_0 \rightarrow {}^7F_2$	0.0033	0	0
$^5D_0 \rightarrow {}^7F_4$	0	0.0023	0
$^5D_0 \rightarrow {}^7F_6$	0	0	0.0003

Table 2. Value of the J-O intensity parameters of Eu^{3+} in SYGO host lattice

Sample	Ω_2 (10^{-19} cm^2)	Ω_4 (10^{-19} cm^2)
SYGO:0.05Eu^{3+}	3.1	1.8

The J – O parameter of SYGO: Eu^{3+} obtained is $\Omega_2 > \Omega_4$, confirming the existence of covalent bonds between Eu^{3+} ion and surrounding ligands, as well as the asymmetry around the metal ion position. . Referring to the parameter $\Omega_{2,4}$ previously published for other oxide matrix networks such as ytrium and germany, it is found that $\Omega_2 > \Omega_4$. This again confirms that a covalent bond exists between the Eu^{3+} ion and the surrounding ligands.

In addition to the value $\Omega_{2.4}$, the radiation conversion rate (A_R), radiation lifetime (τ_R) and luminescence branching ratio (β_R) of SYGO: 0.05Eu^{3+} materials were also determined by Eq. (2) as shown in Table 3.

Table 3. Emission probability (A_R) values, emission cross-section ($\sigma_{\lambda p}$), calculated and experimental values of branch ratio (β), lifetime (τ) and Quantum efficiency ($\eta = \tau_{exp}/\tau_{cal}$) level $^5D_0$ of Eu^{3+}.

$^5D_0 \rightarrow {}^7F_J$	σ (x 10^{-21} cm^2)	β_{exp} (%)	β_{cal} (%)	A_R (s^{-1})	τ_{exp}(s)	τ_{cal}(s)	η (%)
$^5D_0 \rightarrow {}^7F_1$	0.049	0.04	0.03	653.9	0.0019	0.0015	66.7
$^5D_0 \rightarrow {}^7F_2$	2.9	0.66	0.64				
$^5D_0 \rightarrow {}^7F_4$	5.3	0.3	0.33				

The values of β_{cal} and β_{exp} illustrated to the displacements of Eu^{3+} ions. Of all the samples, the values of the branch ratio β_{exp} and β_{cal} of displacement $^5D_0 \rightarrow {}^7F_2$ were the largest. The branching rate of a given displacement is higher than 50%, then it can be used as laser radiation [22]. In the present study, the SYGO:0.05Eu^{3+} sample had $\beta(^5D_0 \rightarrow {}^7F_2) > 60\%$ (Table 3), demonstrating that these materials have promising applications for laser light.

4. Conclusion

We were successfully synthesized SYGO host lattice and SYGO: x mol Eu^{3+} (x=0.01-0.09) phosphors by the sol-gel method. The phase structure of the phosphors was confirmed by Rietveld analysis. The particle size is about 200 nm, and no impurities were detected in the fabricated material. When excited with NUV light (395 nm), the phosphor emits red, peaking at 612 nm. Based on the J-O theory, we have given the parameters and the result is $\Omega_2 > \Omega_4$, confirming the dominant covalent bond. Meanwhile, emission cross-section, branch ratio, and the quantum radiation efficiency of $^5D_0$ were determined. This shows that Eu^{3+} ion will occupy an asymmetric position in the SYGO host and the quantum yield is close to 70%. This work shows an overview of the spectrum properties of Eu^{3+} ions in SYGO host lattice.

Acknowledgments

This research was funded by the Ministry of Education and Training (MOET) under grant number B2021-BKA-05.

References

[1] N. Horiuchi, Light-emitting Diodes: Natural white Light, Nat Photon, Vol 4, 2010, pp. 738-740, http://doi.org/10.1038/nphoton.2010.244.

[2] S. Lee, J. Y. Hong, J. Jang, Performance Enhancement of white Light-emitting Diodes Using an Encapsulant Semi-Solidification Method, J Mater Chem C, Vol 2, 2014, pp. 8525-8531, http://doi.org/10.1039/C4TC01221F.

[3] C. Ruan, X. Bai, C. Sun, H. Chen, C. Wu, X. Chen et al., White Light-emitting Diodes of High Color Rendering Index with Polymer dot Phosphors, RSC Adv., Vol. 108, 2016, pp. 1-6, https://doi.org/10.1039/C6RA20704A.

[4] X. Zhang, M. Gong, Single-phased White-light-emitting $NaCaBO_3$: Ce^{3+}, Tb^{3+}, Mn^{2+} Phosphors for LED Applications, Dalton Trans, Vol. 43, 2014, pp. 2465-2472, https://doi.org/10.1039/C3DT52328D.

[5] S. Lee, S. Y. Seo, Optimization of Yttrium Aluminum Garnet: Ce^{3+} Phosphors for white Light-Emitting Diodes by Combinatorial Chemistry Method, J Electrochem, Soc, Vol. 149, No. 11, 2002, pp. J85-J88, http://doi.org/10.1149/1.1511755.

[6] C. R. Ronda, Luminescence from Theory to Applications Wiley Publication, Weinheim, Germany, 2008.

[7] S. Neeraj, N. Kijima, A. K. Cheetham, Novel Red Phosphors for Solid-State Lighting: The System $NaM(WO_4)_{2-x}(MoO_4)_x$:Eu^{3+} (M Gd, Y, Bi), Chem. Phys. Lett., Vol 387, 2004, pp. 2-6, https://doi.org/10.1016/j.cplett.2003.12.130.

[8] O. Lipina, L. Surat, M. Melkozerova, A. Tyutyunnik, I. Leonidov, V. Zubkov, Synthesis, Crystal Structure and Luminescence Properties of $CaY_2Ge_3O_{10}$:Ln^{3+}, Ln = Eu, Tb, Opt. Spectrosc., Vol. 116, No. 5, 2014, pp. 695–699, https://doi.org/10.1134/S0030400X14050130.

[9] Y. Liu, J. Hao, W. Zhuang, Y. Hu, Structural and Luminescent Properties of Gel-combustion Synthesized Green-Emitting $Ca_3Sc_2Si_3O_{12}$: Ce^{3+} Phosphor for Solid-state Lighting, J. Phys. D: Appl. Phys., Vol 42, 2009, pp. 1-6, http://doi.org/10.1088/0022-3727/42/24/245102.

[10] D. Chen, Y. Chen, H. Lu, Z. Ji, A Bifunctional Cr/Yb/Tm:$Ca_3Ga_2Ge_3O_{12}$ Phosphor with Near-Infrared Long-Lasting Phosphorescence and Upconversion Luminescence, Inorg. Chem., Vol 53, 2014, pp. 8638–8645, https://doi.org/10.1021/ic501238u.

[11] D. Uhlich, J. Plewa, Thomas Ju¨ Stel, Phase Formation and Characterization of $Sr_3Y_2Ge_3O_{12}$, $Sr_3In_2Ge_3O_{12}$, and $Ca_3Ga_2Ge_3O_{12}$ Doped by Trivalent Europium, Journal of Luminescence, Vol. 128, 2008, pp. 1649-1654, https://doi.org/10.1016/j.jlumin.2008.03.022.

[12] S. K. Hussain, L. K. Bharat, D. H. Kim, J. S. Yu. L. K. Bharat, D. H. Kim, J. S. Yu, Facile Pechini Synthesis of $Sr_3Y_2Ge_3O_{12}$:Bi^{3+}/Eu^{3+} Phosphors with Tunable Emissions and Energy Transfer for WLEDs, Journal of Alloys and Compounds, Vol. 703, 2017, pp. 361-369, http://doi.org/10.1016/j.jallcom.2017.01.345.

[13] S. K. Hussain, J. S. Yu, Broad Red-emission of $Sr_3Y_2Ge_3O_{12}$:Eu^{2+} Garnet Phosphors under Blue Excitation for Warm WLED Applications, RSC Adv., Vol. 7, 2017, pp. 13281-13288, https://doi.org/10.1039/C6RA28069B.

[14] M. G. Brik, Ž. M. Antić, K. Vuković, M. D. Dramićanin, Judd–Ofelt Analysis of Eu^{3+} Emission in TiO_2 Anatase Nanoparticles, Mater. Trans., Vol. 56, No. 9, 2015, pp. 1416-1418, http://doi.org/10.2320/matertrans.MA201566.

[15] A. You, M. A. Y. Be, I. In, NMR-Relaxation Mechanisms of O17in Aqueous Solutions of Paramagnetic Cations and the Lifetime of Water Molecules in the First Coordination Sphere, J. Chem. Phys, Vol. 37, No. 2, 1962, pp. 307-320, https://doi.org/10.1063/1.1701321.

[16] E. Ghoul, J. Omri, K. G. Lopera, S. A. E. Mir, Sol–gel Synthesis, Structural and Luminescence Properties of MT-Doped SiO_2/Zn_2SiO_4 Nanocomposites, Optical Materials, Vol 36, 2014, pp. 1034-1039, https://doi.org/10.1016/j.optmat.2014.01.019.

[17] I. M. Nagpure, S. J. Dhoble, M. Mohapatra, V. Kumar, S. S. Pitale, O. M. Ntwaeaborwa, H. C. Swart, Dependence of Eu^{3+} Luminescence Dynamics on the Structure of the Combustion Synthesized $Sr_5(PO_4)_3F$ host. Journal of Alloys and Compounds, Vol. 509, 2011, pp. 2544-2551, https://doi.org/10.1016/j.jallcom.2010.11.086.

[18] G. H. Dieke, H. M. Crosswhite, H. Crosswhite (Eds.), Spectra and Energy Levels of Rare Earth Ions in Crystals, Interscience Publishers, Wiley, New York, USA, 1968.

[19] M. H. V. Werts, R. T. F. Jukes, Verhoeven, The emission Spectrum and the Radiative Lifetime of Eu^{3+} in Luminescent Lanthanide Complexes, Physical Chemistry Chemical Physics, Vol. 4, 2002, pp. 1542–1548, https://doi.org/10.1039/B107770H.

[20] S. M. Pardha, U. V. Varadaraju, Photoluminescence Studies on Eu^{2+}-activated Li_2SrSiO_4 a Potential Orange-Yellow Phosphor for Solid-State Lighting, Chemistry of material, Vol. 18, 2006, pp. 5267-5272, https://doi.org/10.1021/cm061362u.

[21] P. Babu, C. K. Jayasankar, Optical Spectroscopy of Eu^{3+} Ions in Lithium Borate and Lithium Fluoroborate Glasses. Physica B: Condensed Matter, Vol. 279, 2000, pp. 262-281, https://doi.org/10.1016/S0921-4526(99)00876-5.

[22] X. Joseph, R. George, S. Thomas, M. Gopinath, M. S. Sajna, N. V. Unnikrishnan, Spectroscopic Investigations on Eu3+ ions in Li–K–Zn Fluorotellurite Glasses, Optical Materials, Vol. 37, 2014, pp. 552–560, http://dx.doi.org/10.1016/j.optmat.2014.07.021.